3164 © 1985 The Chemical Society of Japan Bull. Chem. Soc. Jpn., 58, 3164—3171 (1985) [Vol. 58, No. 11

Activity and Selectivity Regulation of Synthesis Gas Reaction over Supported Ruthenium Catalysts

Kaoru FUJIMOTO,* Tatsuya NOBUSAWA, Takakazu FUKUSHIMA, and Hiro-o TOMINAGA
Department of Synthetic Chemistry, Faculty of Engineering, The University of Tokyo,
Hongo, Bunkyo-ku, Tokyo 113

(Received February 15, 1985)

The catalytic activities of supported ruthenium for synthesis-gas conversion to hydrocarbons was found to be in the following order:

$$TiO_2 > Nb_2O_3 > ZrO_2 > SiO_2 > Ta_2O_5 > Al_2O_3 > V_2O_5 > Mo_3 > WO_3 > MnO_2 > ZnO$$

Turnover frequencies of the supported ruthenium increased with decrease in dispersion of the metal particles for every carrier material. Even the activities per unit weight of metals were higher for low-dispersion ruthenium on Al_2O_3, TiO_2, and ZrO_2. The chain-growth probability of a hydrocarbon product, which is characterized by the Schulz-Flory distribution, increased markedly with decrease in the metal dispersion irrespective of the carrier material. The catalytic activity of ruthenium particles with a dispersion level of 0.7 or higher reached a ceiling level at about 0.5 MPa, whereas that of low dispersed ruthenium increased almost linearly with an increase in reaction pressure (up to at least 2.0 MPa).

A supported ruthenium catalyst is one of the most active and promising catalysts for producing liquid hydrocarbons from synthesis gas.[1–3] Hydrocarbon products of Fischer-Tropsch (F-T) synthesis on supported ruthenium catalysts have been known to follow the Schluz-Flory distribution.[4,5] One of the most important targets regarding catalyst preparation for producing a liquid hydrocarbon by F-T synthesis is to control the probability of hydrocarbon chain growth. A maximization of the formation of C_5 to C_{20} hydrocarbons is especially important. Vannice *et al.*[3] and Kikuchi *et al.*[6] have reported that activities of supported ruthenium catalysts are markedly influenced by carrier materials and that, especially, Ru/TiO_2 is one of the most active and chain-growing catalysts. The activity and selectivity of a ruthenium catalyst are also influenced by the sizes of supported metals.[4–6] King has claimed that although the turnover frequency (TOF) of a synthesis-gas reaction increases with a decrease in the metal dispersion, no consistent relationship between the chain-growth probability of the product hydrocarbon and the dispersion exists.[7] Kellner and Bell have reported that the turnover frequency of a reaction on alumina-supported ruthenium catalysts under atmospheric conditions decreases moderately with an increasing dispersion (up to 0.7). The decrease is above 0.7, but neither the chain-growth probability nor the olefin-to-paraffin ratio is affected.[4]

The activity and selectivity of ruthenium catalysts should be determined under pressurized conditions using a synthesis gas of normal composition in order to determine the real performances of the F-T reaction, since they are very sensitive to these conditions.[1,2] In both of the studies mentioned above, the dispersions of supported ruthenium were controlled by regulating the ruthenium loading. This method is quite powerful for controlling metal dispersion; however, it has a disadvantages that the particle sizes are widely distributed.[8] Also, the range of the dispersion controlled by this method is not wide enough.

The present authors have developed a simple method for regulating the dispersion level of a supported ruthenium catalyst with constant loading and with the same source material and have shown that both activity and selectivity are influenced by either the carrier materials or the dispersion level of ruthenium.[5]

In the present work, the effects of carriers and the sizes of metal particles of supported ruthenium catalysts on the activity, selectivity, and other catalytic features (characterized by the CO conversion rate per weight of a catalyst, turn-over frequency, chain-growth probability, methane selectivity and pressure dependence) were studied under conditions normally utilized for F-T synthesis.

Experimental

Catalyst Preparation and Dispersion Measurements. All catalysts used in the present study contained 2 wt% of ruthenium. TiO_2 was obtained by the hydrolysis of titanium isopropoxide ($[(CH_3)_2CHO]_4Ti$), followed by calcining at 723 K for 3 h. This gave anatase type TiO_2. WO_3 and MoO_3 were prepared through the calcination (in air at 773 K for 7 h) of ammonium tungstate ($(NH_4)_2WO_4$) and ammonium molybdate ($(NH_4)_2 MoO_4$), respectively. Alumina–magnesia(Al_2O_3–6MgO) was prepared by the calcination (in air at 723 K for 1 h) of a commercially available Al–Mg hydroxycabonate ($Mg_6Al_2(OH)_{16}CO_3$). Other metal oxides were used as received after calcining in air at 723 K for 1 h. SiO_2 (Aerosil-380) was obtained from Japan Aerosil Co. (380 m^2/g). A γ-Al_2O_3 (220 m^2/g) was prepared by hydrolyzing aluminium isopropoxide and calcining in air at 873 K for 3 h. Supported ruthenium catalysts were prepared by impregnating the carriers with $RuCl_3\cdot 3H_2O$ from its aqueons solutions, drying at 353 K and then drying overnight at 393 K in an air oven. These catalysts were represented as H-(Highly-dispersed) catalysts.

Another group of catalysts represented as L-(Low-dispersed) catalysts were prepared by calcining H catalysts in air at 673 K for 3 h before reduction. The catalyst precursors were molded to granules (20—40 mesh) under pressure. The catalysts were activated in situ by reducing in flowing hydrogen at 453 K for 1 hr and then at 673 K for 2 h.

The chemisorption of CO was measured at room temperature using a flow-through cell connected to a glass vacuum system. A catalyst sample was first activated *in situ* as described above and then evacuated at 723 K for 3 h. The amount of desorped CO was determined as the difference between the first isotherm and the second isotherm which was measured following to evacuation for 30 min at room temperature after the first isotherm measurement. Metal dispersion was calculated assuming that one CO molecule was chemisorbed by one surface ruthenium atom.

Synthesis Gas Reaction and Product Analysis. Synthesis gas reactions were conducted in a flow-type fixed-bed reaction apparatus under pressurized conditions. A stainless-steel tube (inner diameter 8 mm, outer diameter 10 mm) was used as a reactor. The details of this apparatus has been described elswhere.[9] When highly active catalysts were used, they were diluted by α-Al_2O_3 (surface area<2 m^2/g) granules with the same size (20/40 mesh) in order to produce an even temperature profile over the catalyst bed (within 2K).

Activities and selectivities of the ruthenium catalysts were measured under the following reaction conditions: 503 K, 2.03 MPa, $H_2/CO=2$. The time factor (W/F) was adjusted to produce about 10% CO conversion.

Synthesis gas ($H_2/CO=2$) was introduced into the reactor after being purified by being passed through a series of silica-gel and activated charcoal columns. All products effluted from the catalyst bed were withdrawn in gaseous states from the high-pressure zone and were analyzed on-line by gas chromatographs. Hydrocarbons trapped in the catalyst bed during the reaction were extracted *in situ* with hot toluene for 1 h after a reaction was completed to be analyzed. CO, CH_4, and CO_2 were analyzed using an activated charcoal column. C_1–C_5 hydrocarbons were analyzed with a Porapak Q column, C_4–C_{20} hydrocarbons were analyzed with a Silicone SE-30/Chromosorb 101 column and C_{10}–C_{45} hydrocarbons were analyzed with a Dexil 300 GC column, respectively.

In all that follows, catalyst activity is defined by the equation:

Activity=$(CO_{in}-CO_{out})/W$ where CO_{in} and CO_{out} are the flow rates of carbon monoxide which enter and exit the reactor (moles/hour), respectively and W is the catalyst weight (gram).

Table 1. CO Chemisorption, dispersion and specific activity of supported ruthenium catalyst[a)]

Carrier	CO_{ch}[b)]	D_{Ru}[c)]	N_{CO}[d)]	α[e)]
	μ-mol/g-cat	%	10^{-3}/s	
γ-Al_2O_3(H)	*225*	*58.1*	*32*	*0.64*
γ-Al_2O_3(L)	30.0	15.2	182	0.88
TiO_2(H)	174.3	88.7	42	0.62
TiO_2(L)	50.0	30.1	355	0.82
SiO_2(H)	51.4	26.4	143	0.66
SiO_2(L)	10.0	5.1	278	0.82
ZrO_2(H)	20.0	10.3	520	0.77
ZrO_2(L)	12.9	6.6	862	0.86
Nb_2O_5	44.7	22.6	390	0.73
Ta_2O_5	19.8	10.0	327	0.79
V_2O_5	144.9	73.2	37	0.65
MoO_3	124.9	63.1	30	0.66
WO_3	87.7	44.3	12	0.73
MnO_2	89.1	45.0	5.0	0.57
ZnO	40.9	20.7	11	0.66
$Al_2O_3\cdot 6MgO$	110.5	55.8	2.8	0.56

a) 2 wt% Ru on carrier. b) CO chemisorption at room temperature. c) Dispersion of ruthenium. d) Turnover frequency. e) Chain growth probability.

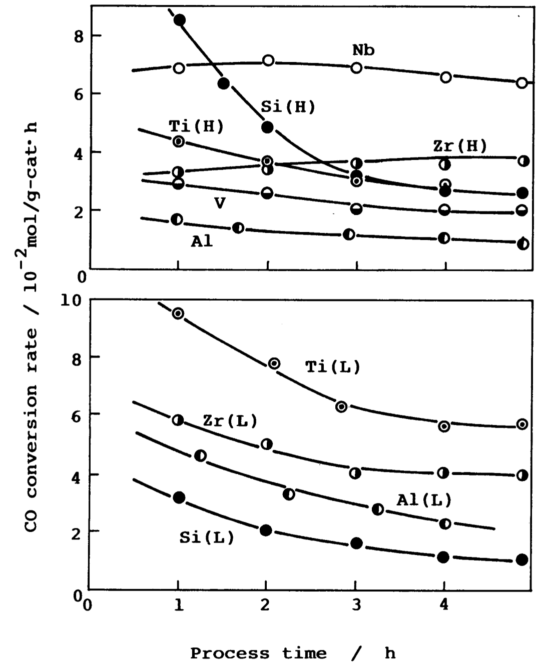

Fig. 1. Change in catalytic activity of supported ruthenium catalysts. Temperature: 503 K, Pressure: 2.03 MPa, H_2/CO: 2/1 mole ratio.

Results and Discussion

Metal Dispersion. Table 1 shows the amount of CO chemisorption, metal dispersion, catalyst activities and turn-over frequencies. The dispersion level of supported ruthenium prepared without air calcination is distributed between 10 and 90%. Obviously, the dispersions of ruthenium on each of the four carriers (ZrO_2, SiO_2, Al_2O_3, TiO_2) were lowered due to air calcination prior to reduction. Since ruthenium chloride has been proven by our experiment to be converted to ruthenium oxide during air calcination, it can move easily on the carrier and aggregate into large particles as expected due to its high sublimation characteristics.

Characteristic Features of Synthesis-gas Reaction. As demonstrated in Fig. 1, the activities of most catalysts, expressed by CO conversion rates, decreased with the processing time. Since deactivated catalysts restored their activities upon being treated with hydrogen at 673 K, the deactivation can be attributed to carbon deposition or an accumulation of wax on the catalysts. The activities and selectivities were expressed by average values which were measured between 4 and 5 h after starting.

The product hydrocarbon, eluted from the catalyst bed in a gaseous state, was characterized by the fact that hydrocabons higher than C_{15} are quite small, as demonstrated in Fig. 8. This was the same even with the L-catalysts whose chain-growth ability was high. It was caused by a trapping of high-boiling-point hydrocarbons in the catalyst bed.[5] A large amount of waxy hydrocarbon was extracted with hot toluene after the synthesis-gas reaction. By combining the extracted products with the gaseous products, the ratio of the amount of recovered hydrocarbons to the amount of consumed carbon monoxide (on carbon base) increased from 35 to 88% (for Ti–L-catalyst) and from 63 to 91% (Ti–H catalyst), respectively. The total hydrocarbon distributions, thus obtained, showed smooth profiles distributed from C_1 to C_{40}, or higher (Figs. 2 and 3). The distributions fit the Schulz-Flory equation very well as demonstrated by Figs. 4 and 5. It is clear from

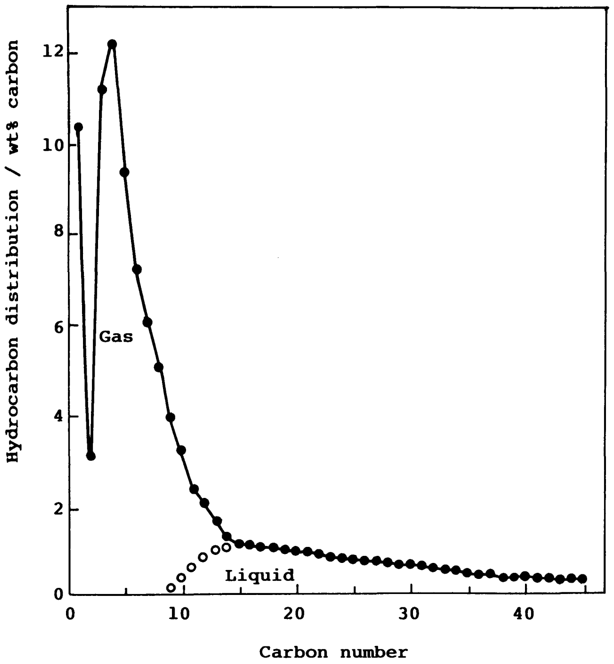

Fig. 2. Hydrocarbon distribution of the products on Ti–H catalyst. Temperature: 503 K, Pressure: 2.03 MPa, H_2/CO : 2/1 mol ratio.

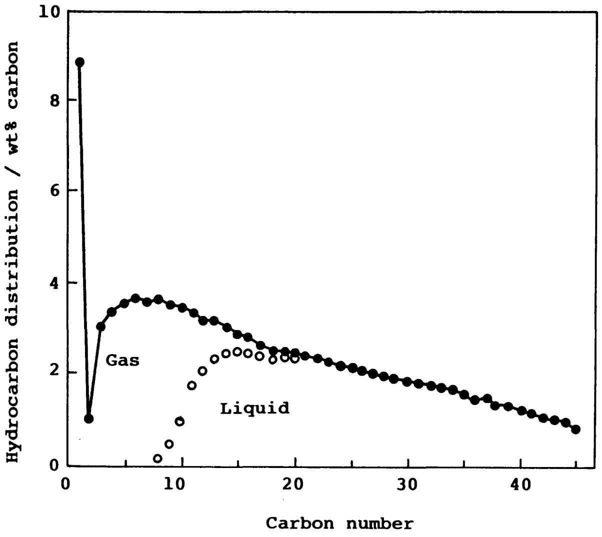

Fig. 3. Hydrocarbon distribution of the products on Ti–L catalyst. Temperature: 503 K, Pressure: 2.03 MPa, H_2/CO : 2/1 mole ratio.

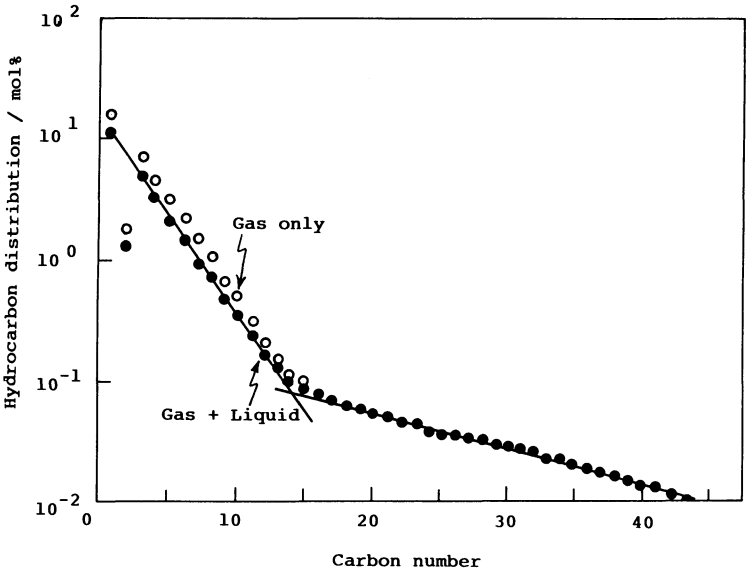

Fig. 4. Schluz-Flory plot of the product on Ti–H catalyst. Same product as shown in Fig. 2.

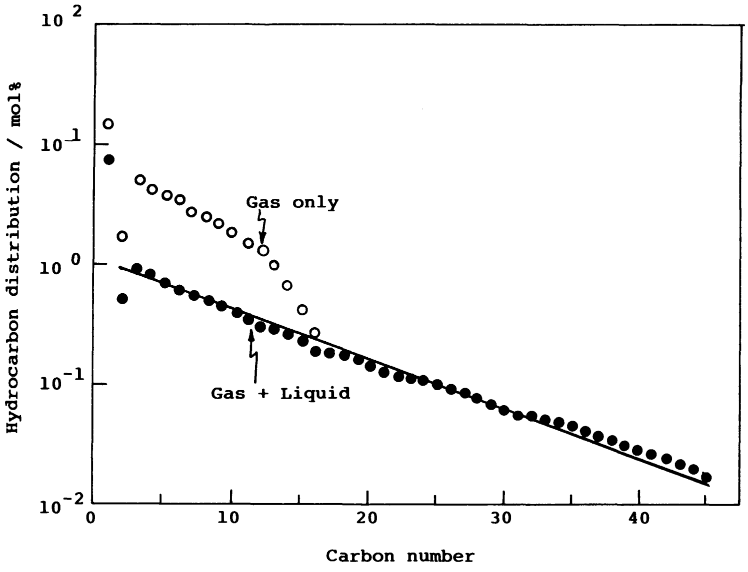

Fig. 5. Schluz-Flory plot of the product on Ti–L catalyst. Same product as shown in Fig. 3.

the data in Fig. 3 that the chain-growth probability (α value), which is determined from the distribution of gaseous hydrocarbons, agrees well with that obtained from the combined product. The α values of other catalysts were determined from the distribution of gaseous products. It is also worth while to note that the Schulz-Flory plot for a Ti–H catalyst can be expressed by two straight lines, whereas that of a Ti–L catalyst can be expressed by one straight line. This phenomenon will be discussed in the later chapter.

Controlling Factors of Catalyst Activity. The conversion levels, catalytic activities, methane selectivities, olefin content of products and chain-growth probabilities are shown in Tables 1 and 2. Although metal loadings are the same for all catalysts, metal dispersions are distributed from 5 to 89% and the activity per unit weight of catalysts are distrubued over a range of about 60 by factor. Figure 6 shows the relationship between ruthenium disperion and the turnover frequency (TOF). It is clear that the TOF is controlled not only by carrier materials, but also by the ruthenium dispersion. Catalysts can be classified into 3 groups: (1) Low dispersion-high TOF, (2) high dispersion-low TOF, and (3) low dispersion-low TOF. It is also demonstrated that a decrease in the dispersion by air calcination causes an increase in the TOF without exception. Similar facts have already been pointed out by King regarding methane synthesis.7) or by Kikuchi *et al.*6) for CO

TABLE 2. PERFORMANCES OF CO HYDROGENATION ON SUPPORTED RUTHENIUM CATALYSTSa)

Carrier	W/Fb) g-cat·h/mol	CO conv. %	CH_4 select C-wt%	Olefine content C_2–C_{10}, mol%	Activityc) molCO/g-cat·h
γ-Al_2O_3 (H)	4.9	4.8	12.0	45.9	0.97
γ-Al_2O_3 (L)	2.5	7.1	5.0	46.9	1.97
TiO_2 (H)	2.5	6.6	8.4	61.4	2.65
TiO_2 (L)	2.5	14.1	7.3	34.5	6.40
SiO_2 (H)	2.5	6.6	24.5	38.8	2.64
SiO_2 (L)	2.5	2.4	13.2	36.1	1.00
ZrO_2 (H)	2.5	9.3	18.7	24.8	3.74
ZrO_2 (L)	2.5	10.2	8.0	30.2	4.00
Nb_2O_5	2.5	16.7	12.9	24.1	6.27
Ta_2O_5	11.2	27.8	7.1	24.1	2.33
V_2O_5	2.5	5.2	10.1	65.3	1.94
MoO_3	11.0	16.0	13.4	5.4	1.35
WO_3	22.4	9.2	10.9	0.9	0.39
MnO_2	22.0	3.9	57.3	24.9	0.16
ZnO	21.5	3.6	5.1	43.4	0.16
Al_2O_3·6MgO	22.7	2.4	28.8	33.1	0.11

a) 2 wt% Ru on carrier. b) Contact time. c) Catalytic activity.

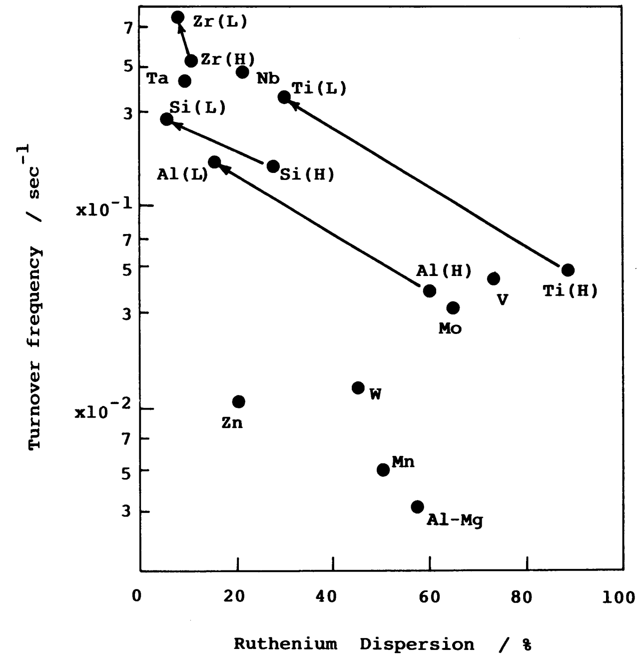

Fig. 6. Turnover frequency *vs.* ruthenium dispersion of supported ruthenium catalyst. Temperature: 503 K, Pressure : 2.03 MPa, H_2/CO : 2/1 mole ratio.

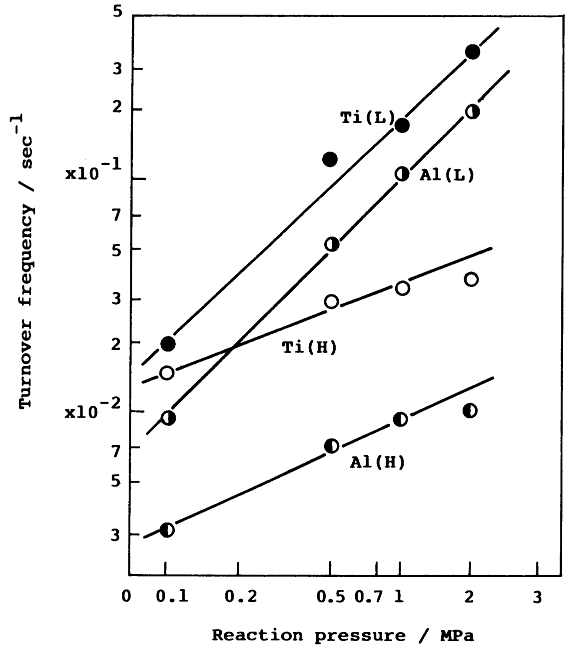

Fig. 7. Pressure dependency of the Ti–H, Ti–L, Al–H, and Al–L catalysts. Temperature: 503 K, H_2/CO: 2/1 mole ratio.

hydrogenation and by Kellner *et al.*[4] for the atomospheric Fischer-Tropsch synthesis. Not only the TOF but also activities per unit weight of ruthenium are higher for L-catalysts than for H-catalysts (Table 2). Thus, the fairly poor dispersion (less than 30%) of ruthenium is favored for the high activity of F-T synthesis. The reason for the high activity of the low-dispersed ruthenium has been discussed by Kellner *et al.*[4] however, the real reason has not been made clear yet. The L-catalyst exhibits, as will be shown in the later chapter, high activity under high reaction pressures.

On a similar dispersion basis, ruthenium showed a high activity when it was supported on Nb_2O_5, TiO_2, ZrO_2, SiO_2, or Ta_2O_5. ZnO, MnO_2, WO_3, and Al-Mg oxide showed poor abilities as carriers of ruthenium. Thus, it can be concluded that the selection of a carrier is also one of the essential factors in effecting catalytic activity. The effect of carrier materials on catalytic activity may be ascribed not only to the difference in metal dispersion, but also to some interaction between the carrier and the metal. In fact, by using carriers such as Nb_2O_5, TiO_2, Ta_2O_5, and V_2O_3, known to exhibit a SMSI effect,[10–12] highly active catalysts could be prepared.

Pressure Characteristics. It was also found that the degree of ruthenium dispersion affects the pressure characteristics of catalytic activity. It is very clear from Fig. 7 that the catalytic activity of a TiO_2-supported H-catalyst (Ti–H catalyst) increases markedly with an increase in pressure from 0.1 MPa to 0.51 MPa. However, above this the increase in the activity is quite small. The activity of a Ti–L catalyst increases almost linearly up to a pressure of 2.03 MPa. Thus, the activity of a H-catalyst is higher than that of a L-catalyst under atmospheric pressure, the reverse is true above 1.01 MPa. Not only the TiO_2 supported catalyst, but also the Ru/Al_2O_3 catalysts exhibit the same characteristics.

As can be seen in Fig. 7, the average reaction orders with respect to the total pressure at $H_2/CO=2/1$ were determined to be about 1 for both Ti–L and Al–L catalysts while those of Ti–H and Al–H catalysts are 0.4 and 0.6, respectively. It has been reported that the reaction order of the F-T reaction over Ru/Al_2O_3 catalysts are close to or higher than 1.0 with respect to hydrogen, whereas it is zero or negative with respect to carbon monoxide.[13,14] As the reaction order with respect to the total pressure is the sum of the orders with respect to the partial pressures of carbon monoxide and hydrogen, the low reaction order of an H-catalyst may due to a negative reaction order with respect to carbon monoxide. However, the details must be determined in further studies.

Controlling Factors of Product Selectivity.

a. Chain Growth. Figure 8 shows carbon number distributions of gaseous products under a standard condition with the above-mentioned 4 types of H- and L-catalysts. It is obvious that the distribution is less steep for L-catalysts than for H-catalysts, without exception. This indicates that the chain-growth probability is higher for L-catalysts. Figure 9 exhibits a clear inverse relationship between the dispersion and the growth probability, irrespec-

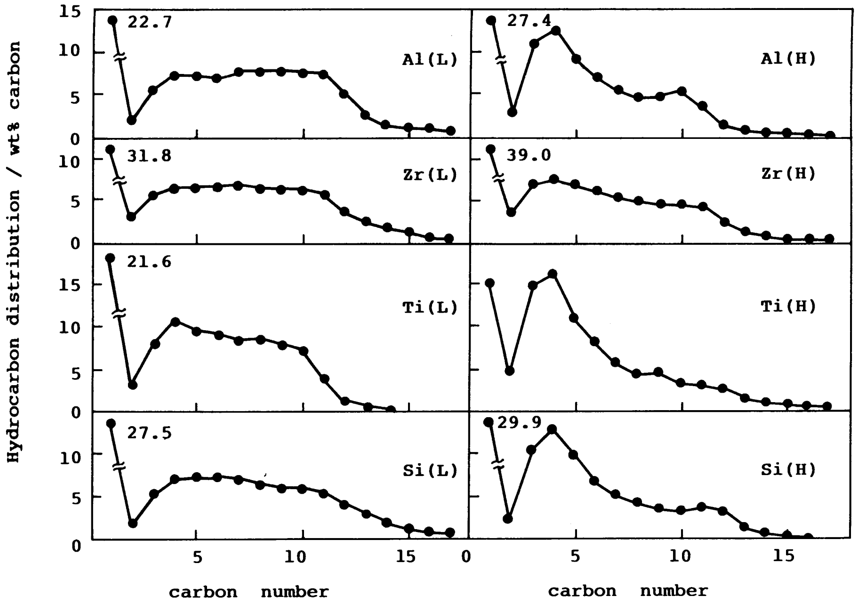

Fig. 8. Carbon number distribution of gaseous produts on L and H type ruthenium catalysts. Temperature: 503 K, Pressure: 2.03 MPa, H_2/CO : 2/1 mole ratio.

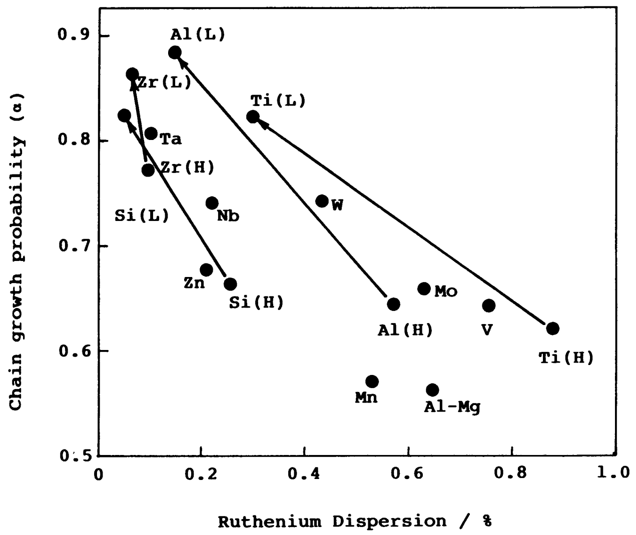

Fig. 9. Chain growth probability *vs.* ruthenium dispersion of supported ruthenium catalysts. Temperature: 503 K, Pressure: 2.03 MPa, H_2/CO : 2/1 mole ratio.

tive of carrier materials. It is also apparent that the calcination of the supported ruthenium chloride in air prior to hydrogen reduction caused the growth of ruthenium particles as well as the increase in the chain-growth probability. The results coincide well with that of Jacobs *et al.*[21], namely the values of α are mostly higher than 0.8 when the dispersion level is lower than 0.3. Thus, the regulating the dispersion level of ruthenium is one of the most effective methods for controlling the activity and the chain-growth ability of a catalyst.

Carrier material is also an important factor for regulating the α value. Ruthenium metals supported on TiO_2, Al_2O_3, or WO_3 exhibit high α values for a similar dispersion level. Among them, TiO_2 is an excellent carrier for a ruthenium catalyst with either CO conversion or carbon–carbon bond formation, as has already been shown.[16,17] However, supported ruthenium particles with the dispersion levels of 10% or lower exhibit high chain-growth probabilities irrespective of the carrier materials. This fact suggests that the carrier effect is reduced at low dispersion since there is a small contact area between ruthenium particle and the carrier surface.

b. Deviation from Schulz-Flory Distribution. Several examples have been reported where products on supported ruthenium catalysts do not follow the S-F distribution.[18–20] Jacobs *et al.* suggested that the unique distributions can be well simulated by assuming that the maximum carbon number of product hydrocarbon depends upon the sizes of metal particles.[21] In the present work, the S-F plots (Figs. 4 and 5) of products show that the distribution for an H-catalyst can be expressed by two straight lines, wheares that for an L-catalyst is well approximated by one straight line. The values of α obtained from the slopes of the plots are 0.87 for the Ti–L-catalyst, while 0.65 and 0.8 for the Ti–H-catalyst, respectively. The approximation using two staight lines had been also reported.[22]

The present authors explain the phenomenon as follows: It is common that a supported metal catalyst has a wide distribution regarding the size of metal particles when it is prepared by the impregnation method.[8] Thus, an H-catalyst should have particles with both "high" and "low" dispersions. The critical dispersion level of "high" and "low" is

TABLE 3. ISOPARAFFIN FORMATION[a)]

Catalyst	Ru/MoO_3	Ru/WO_3	Ru/TiO_2+WO_3[b)]	Ru/TiO_2+WO_3[b,c)]
Time Factor (W/F)	11.0	22.4	12.5	12.5
CO conversion/%	16.0	9.2	10.7	18.6[c)]
Hydrocarbon distribution/c-wt%				
C_1	24.8	12.4	16.1	18.1
C_2	6.6	3.3	5.3	4.3
C_3	10.8	5.6	10.2	9.0
C_4	11.8(0.4)[d)]	15.5(2.8)[d)]	15.5(>0.1)[d)]	15.8(0.2)[d)]
C_5	7.6(0.8)	15.4(50.4)	14.7(0.4)	13.2(1.0)
C_6	9.4(1.3)	13.8(8.2)	9.3(0.4)	10.6(1.7)
C_7	6.6(1.3)	12.2(10.0)	7.3(0.5)	8.4(2.0)
C_8	5.1(1.3)	9.9(8.0)	6.9(0.4)	6.8(3.0)
C_9	4.0(1.4)	5.7(8.5)	4.7(0.6)	5.6(3.7)
C_{10}^+	13.2	6.0	10.1	9.8

a) Temperature: 230 °C, Pressure: 21 bar, H_2/CO: 2/1. b) Ru/TiO_2: 20 wt%, WO_3: 80 wt%. c) 250 °C. d) Branched product/normal product.

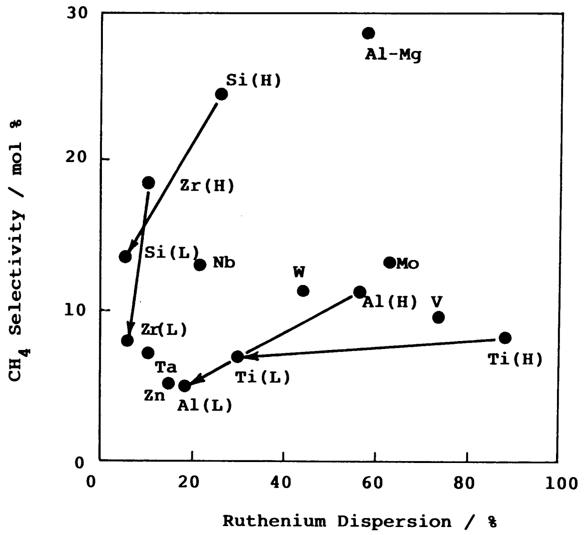

Fig. 10. Methane selectivity *vs.* ruthenium dispersion of supported ruthenium catalysts. Temperature: 503 K, Pressure : 2.03 MPa, H_2/CO : 2/1 mole ratio.

estimated to be about 30%, as described above. This classification is based on our finding that the chain-growth ability of a supported ruthenium catalyst is definitely divided at 30% of the dispersion.[23)] The products on the high- and low- dispersion particles supported on TiO_2 should have the α values of 0.65 and 0.87, respectively, under the conditions adopted. On the other hand, all metal particles on the Ti–L-catalyst should have a dispersion lower than 30%. Since smaller particles can easily aggregate to become large particles, due to sintering during air calcination,[8)] all products on these particles must have a chain-growth probability of 0.87.

c. Methane Selectivity. Points on plots of CH_4 selectivity *vs.* dispersion are scattered widely (Fig. 10). This suggests that the relationship between them is poor. However, for each set of the four carriers (TiO_2, Al_2O_3, ZrO_2, SiO_2) a decrease in the dispersion is necessarily accompanied by a decrease in the CH_4 selectivity. So long as the decrease in the dispersion brings about an increase in the chain-growth probabbility, as pointed out in the present paper, a decrease in the CH_4 selectivity can be expected due to the S-F equation. However, since the drastic decrease in the CH_4 selectivity (about 50%) for Ru/SiO_2 and the Ru/ZrO_2 catalysts is unable to be explained by the S-F theory, some unknown dispersion effect remains to be accounted for. Also, carrier materials, themselves, are the controlling factors of CH_4 selectivity. SiO_2, ZrO_2, Al-MgO_x, and Nb_2O_5 are favored for CH_4 formation whereas V_2O_5, TiO_2, Al_2O_3, and ZnO are effective for suppressing CH_4 formation. Thus, it is concluded a low-dispersion ruthenium catalyst supported on Al_2O_3 or TiO_2 is favored for selectively producing liquid hydrocarbons.

d. Isoparaffin Formation. It is interesting to note that with the MoO_3- and the WO_3- supported catalysts, methane selectivities are fairly low in spite of the low olefin contents in the products. Also, the high selectivities of isoparaffins are obtained, which are scarcely observed in products with other catalysts. These phenomena were especially marked in the case of the WO_3 carrier. As shown in Table 3, the ratio of branched paraffins to normal paraffins (i/n ratio) in hydrocarbons from C_4 to C_{10} is higher than 20 (in total). Isoparaffin formation was also observed (to some extent) when a mixed catalyst consisting of 2 wt% Ru/TiO_2 and WO_3 was subjected to a synthesis-gas reaction. The i/n ratio increased with an increased reaction temperature as demonstrated in Table 3. Isoparaffin formation could be attributed to the acidic character of MoO_3 and WO_3,[7)] which isomerize n-olefins produced on the ruthenium metal to isoolefins which are then hydrogenated to isoparaffins on the carriers or on the ruthenium.

Conclusion

It has been found that the specific activity of supported ruthenium for a synthesis-gas reaction is determined by both carrier materials and ruthenium dispersion, and the selectivity (carbon number distribution of product hydrocarbon) is essentially determined by the dispersion or particle-size distribution, but rather independent of the carrier.

Carrier materials affect both ruthenium dispersion and its catalytic activity. In more detail,

1) Carrier materials which are effective for giving small metal particles are V_2O_5, TiO_2, and Al_2O_3.

2) ZrO_2, SiO_2, TiO_2, and Nb_2O_3 promote the catalytic activity of ruthenium on them.

Effects of ruthenium dispersion on its catalysis are summarized as:

1) The specific activities of supported ruthenium catalysts increase markedly as the dispersion decreases, irrespective of the carrier materials.

2) Low-dispersion ruthenium exhibits a higher chain-growth probability, which is little affected by carrier materials.

3) The chain-growth probability is not uniform for a highly dispersed catalyst, which is suggested to be attributed to the wide distribution of particle sizes.

4) Catalytic activities of low-dispersion catalysts increase almost linearly up to a pressure at about 2.03 MPa. However, those of highly dispersed catalysts level off at around 1.01 MPa.

5) Isoparaffins are formed with high selectivities on MoO_3 and WO_3 supported catalysts. It is suggested that this is caused by their acid character.

References

1) F. S. Karn, J. F. Shultz, and R. B. Anderson, *Ind. Eng. Chem. Prod. Res. Dev.*, **4**, 265 (1965).

2) H. Shulz, "Chemierohstoffe aus Kohle" ed by J. Farbe, George Thieme Verlag, Stuttgart, (1977) pp. 334—355.

3) M. A. Vannice, *J. Catal.* **37**, 449 (1975).

4) C. S. Kellner and A. T. Bell, *J. Catal.* **71**, 288 (1981).

5) T. Fukushima, T. Nobusawa, K. Fujimoto, and H. Tominaga, *Nippon Kagaku Kaishi*, **1982**, 206.

6) E. Kikuchi, H. Nomura, M. Matsumoto, and Y. Morita, *App. Catal.*, **7**, 1 (1983).

7) D. L. King, *J. Catal*, **51**, 386 (1978).

8) J. R. Anderson, "Structure of Metallic Catalysts" Academic Press (1975).

9) K. Fujimoto, Y. Kudo, and H. Tominaga, *Nippon Kagaku, Kaishi*, **1982**, 207.

10) S. J. Tauster, S. C. Fung, and R. L. Garten, *J. Am. Chem. Soc.*, **100**, 170 (1978).

11) S. J. Tauster and S. C. Fung, *J. Catal*, **55**, 29 (1978).

12) K. Foger, *Catalysis, Science and Technology*, **6**, Springer Verlag (1984), p. 227.

13) M. A. Vannice, *Catal. Rev. -Sci. Eng*, **14**, 153 (1976).

14) R. B. Anderson, in "The Fischer-Tropsch Synthesis," Academic Press, (1984) p. 116.

15) K. Fujimoto, M. Kameyama, and T. Kunugi, *J. Catal*, **61**, 7 (1980).

16) M. A. Vannice and R. L. Garten, *J. Catal*, **56**, 236 (1979).

17) M. A. Vannice and R. L. Garten, *J. Catal*, **66**, 242 (1980).

18) J. R. Madon, *J. Catal*, **57**, 183 (1979).

19) Y. Okamura, Y. Iwasawa, K. Domen, and T. Onishi, 49th National Meeting of the Chemical Society of Japan, Tokyo, April 1984, Abstr., No. 1P05.

20) H. H. Nijs, P. A. Jacobs, and J. B. Uytterhoeven, *J. Chem. Soc., Chem. Commun.*, **1979**, 180.

21) H. H. Nijs and P. A. Jacobs, *J. Catal.*, **65**, 328 (1980).

22) C. N. Satterfield, G. A. Huff, and R. Summerhayes, *J. Catal.*, **80**, 486 (1983).

23) K. Fujimoto, M. Miyauchi, and H. Tominaga, 49th National Meeting, Japan Catalysis Society (1984).